Civil Engineering and Architecture 10(4): 1574-1589, 2022
DOI: 10.13189/cea.2022.100427 http://www.hrpub.org

The Behavior of Interior Beam-Column Joint Models Using Self-Compacting Concrete with Variations of Shear Reinforcement Subjected to Cyclic Lateral Loads

Siti Aisyah Nurjannah, Saloma*, Yakni Idris, Arie Putra Usman, Ika Juliantina, Christine Aprilia

Department of Civil Engineering, Faculty of Engineering, Sriwijaya University, Indonesia

Received March 23, 2022; Revised April 29, 2022; Accepted May 28, 2022

Cite This Paper in the following Citation Styles

(a): *[1] Siti Aisyah Nurjannah, Saloma, Yakni Idris, Arie Putra Usman, Ika Juliantina, Christine Aprilia , "The Behavior of Interior Beam-Column Joint Models Using Self-Compacting Concrete with Variations of Shear Reinforcement Subjected to Cyclic Lateral Loads," Civil Engineering and Architecture, Vol. 10, No. 4, pp. 1574-1589, 2022. DOI: 10.13189/cea.2022.100427.*

(b): *Siti Aisyah Nurjannah, Saloma, Yakni Idris, Arie Putra Usman, Ika Juliantina, Christine Aprilia (2022). The Behavior of Interior Beam-Column Joint Models Using Self-Compacting Concrete with Variations of Shear Reinforcement Subjected to Cyclic Lateral Loads. Civil Engineering and Architecture, 10(4), 1574-1589. DOI: 10.13189/cea.2022.100427.*

Abstract The joint of a beam-column is crucial due to the distribution of cyclic lateral loads. Therefore, the joint detail must meet the design requirements of earthquake-resistant structures. Casting work in joint zones where the steel reinforcement spaces are close requires concrete materials that are easy to flow. An alternative to overcome the difficulty is using Self-Compacting Concrete (SCC) material. However, the properties of SCC for beam-column joint structures under earthquake loads still need to be studied further. This study aimed to analyze the behavior of the Interior Beam-Column (IBC) joint using SCC with variations of shear reinforcement subjected to cyclic lateral loads. Three types of shear reinforcement were modeled using numerical analysis. Variations of horizontal and diagonal shear reinforcements were compared to determine the best performance. The SCC-S3 IBC joint model with horizontal and diagonal shear reinforcements achieved the highest lateral forces and resisted compressive and tensile stresses in the largest stress contour and better stiffness degradation than other models of SCC IBC joints. The results showed that the SCC-S3 IBC joint with a combination of horizontal and diagonal shear reinforcements showed the best performance.

Keywords Cyclic Lateral Load, Finite Element Method, Interior Beam-Column Joints, Self-Compacting Concrete

1. Introduction

The well-designed beam-column joints are needed, especially in the area of seismic activities. The joints as connections of beams and columns are crucial because they often fail due to the earthquake loads, then the structure drifts and even collapses [1,2]. The shear forces that occur at the beam-column joints due to earthquakes are greater than in other parts of a structure. It needs an effort to prevent the collapse of beam-column joints by adding the shear reinforcements in the joint zones. The narrow spacing of the shear reinforcement in the joint zones causes difficulties in compacting the concrete; even segregation occurs. The process needs material to flow easily between the steel reinforcement in the joint zone. One of these materials is Self-Compacting Concrete (SCC). It is an innovation of concrete development. This type of concrete does not require a vibrator because of its thinner nature, and then it can flow to fill voids in the formwork and solidify itself [3]. The interest in using Self-Compacting

Concrete as a structural element has increased in recent years [4]. However, the properties and capabilities of SCC as a beam-column joint forming material still require further investigation [5].

This study aimed to analyze the behavior of Interior Beam-Column (IBC) joints under cyclic lateral loads as representative of earthquake loads. There were four numerical models of IBC with three variations of diagonal shear reinforcement in the joint zones that resulted in different performances. The different details of shear reinforcement, including position, space, diameter, yield, and ultimate strengths of the steel bars, affect the beam-column structure performance in resisting lateral cyclic loads [6]. In the analysis, the performance comparison was based on hysteresis curves, ductility, as well as stiffness degradation, and strength degradation of each IBC joint model. The ANSYS software was used to analyze the behavior of structures in resisting cyclic lateral loads. Several models of IBC joints had been inspected using the Finite Element Method (FEM). The structure objects were divided into smaller parts in the analysis, namely elements.

An earthquake is a phenomenon where the earth shakes due to collisions between the earth plates or volcanic activity that can create seismic waves due to the release of energy. These natural disasters often occur at times that are difficult to predict. Some areas lay on active tectonic plates to be included in seismic-risk areas. This condition needs the effort of proper design of the structure to resist earthquake loads. It includes the strength of concrete that depends on various mix designs and the compaction. Normal Concrete (NC) often cannot fill small gaps without vibrating in the casting process. Narrow spaces between bar reinforcements make casting NC that contains aggregates difficult. Self-Compacting Concrete material is often used to solve this problem and ensure the compactness and strength of concrete.

The SCC can bear various environmental and extreme weather conditions. This ability is known as durability. The other superiority of SCC is the ability to flow and solidify itself without vibrating. A high level of workability and flowability minimizes the occurrence of porous and segregation in parts that are difficult to reach, resulting in better compaction in the casting process. The quality of the SCC increases strength to resist compression and durability due to the good homogeneity of the concrete [7].

The steel bar reinforcement plays a role in resisting tensile forces and reducing cracks on concrete. It has high elasticity, ductility, and tensile strength. The value of the tensile strength of steel was obtained from stress-strain testing until the bar break. According to SNI 2847:2019 code [8], the permissible value of the elastic modulus of reinforcement is 200,000 MPa.

The joints connect between the beams and the columns and are parts of the columns, and then their dimensions follow the column dimensions. Every joint of the beam-column requires special attention in structure design to make it resistant to seismic loads. The joints distribute the loads between the beams and columns. Structural failure can occur because of the joint weakness due to the concrete compressive strength, pressure distribution, and reinforcement details. The joints provide shear strength through confinement reinforcement that maintains concrete to withstand the compression and tensile loads. This reinforcement is used to resist tensile forces in a direction perpendicular to the cracks caused by shear forces. The forms of shear reinforcement can be made in horizontal, diagonal, and spiral shapes. The provisions in designing beam-column joints as parts of earthquake-resistant structures emphasize three main aspects. Those are shear strength, the need for transverse reinforcement, and the behavior of beam and column connections that pass through the joints [9].

Cyclic loads represent the earthquake loads through displacement control. The cyclic loads are applied to the specimen on the top column point. The cyclic load is a repeated lateral load that causes fatigue to the structure. Failure occurs if the repeated loads exceed the critical failure level of the structure [10]. The reaction of the structure specimen resulted in hysteretic curves as a correlation of load and displacement. The nature of dynamic loading is loading and unloading [11]. As the horizontal displacement increases, more cracks are formed along with the structural elements, depending on the direction of loading [9]. The propagation of crack causes the degradation of stiffness and strength as well as the number of cyclic loads due to the earthquake. Determination of stiffness from hysteretic curves is derived (1). The stiffness is a ratio of lateral load or lateral strength to displacement [12].

$$K_i = \frac{P_i}{\delta_i} \quad (1)$$

where:

K_i : stiffness (kN/mm)

F_i : lateral load (kN)

δ_i : displacement (mm)

Ductility is the ability of a structure to withstand post-elastic deviation due to repeated earthquake loading. Even though the first yielding occurs due to earthquake loads, the structure must maintain its strength and stiffness to remain standing. According to a code [13], there are three types of ductility: low, moderate, and high, with values of less than 2, 2 to 4, and higher than 4, respectively.

The ductility values can be obtained from the experimental result and finite element analysis. For the preliminary design of structure or study, a finite element analysis using the numeric method is widely used. The FEM was applied by dividing the structure members into smaller elements and solving the equilibrium equations. It makes an option other than experimental testing with faster and relatively exact results. These structures are

numerically modeled as discrete elements connected by nodes in a finite number to represent complex geometric shapes. The result of the FEM is the approximation of the modeled structure node reactions. There is some available software for numerical modeling using FEM. One of them is ANSYS software used in this study [14]. The element modeling is made in such a way as to resemble the original model with a numerical approach. The ANSYS program can analyze the mechanical behavior of the structure under static and dynamic loads, fluid dynamics, and electromagnetics. The Finite Element Method is appropriate when an analytical solution cannot be solved. The work on structural analysis with this method uses the Mechanical Ansys Parametric Design Language (APDL) of ANSYS software. In general, the stages of completion of the FEM using the ANSYS software are as follows [15, 16].

1. Preprocessing

Preprocessing is the initial stage in the finite element method process to define detailed structural element modeling in lines, areas, types of elements, and material properties of the meshing process.

2. Processing

The structural element models are restrained at the processing stage, the loads are applied, and the analysis process is carried out based on the command list.

3. Postprocessing

Postprocessing is the final stage and shows the results of the analysis in the form of tables, and graphs of node-deformation, force on the restraints, stress contours, and crack location.

2. Materials and Methods

This study requires data on the dimension and reinforcement detail of IBC joints, steel bar, Normal Concrete (NC) material properties, and applied axial and lateral cyclic loads. The secondary data used for NC was obtained from the previous research [11]. The concrete compressive strength and modulus of elasticity were 46.5 MPa and 32049 MPa, respectively. The SCC material properties were obtained from previous studies [17] with a compressive strength of 41.813 MPa and elastic modulus of 30391 MPa. The steel bar properties used for modeling were referred to the previous research [11] in Table 1 where f_y and f_u are yield and ultimate strengths, respectively.

Table 1. Steel bar material properties [11]

Strength (MPa)	Type			
	D10	D12	D14	D16
f_y	450	453	443	460
f_u	635	645	668	650

2.1. Interior Beam-Column Joint Model Details

The IBC joint model's detailed dimension was referred to in the previous study [11] and based on a code [18] in Figure 1. The column had a cross-sectional dimension of 300mm×300mm with 8 D16 longitudinal reinforcement and D10-100 stirrup reinforcement. The cross-sectional dimension of the beam was 350 mm × 250 mm with longitudinal reinforcements of 3 D14 at the top, 3 D14 at the bottom, and stirrup reinforcement of D10-100. The modeling of shear reinforcement at the beam-column joint is described in Table 2.

Table 2. Variation of shear reinforcement

Concrete Material	Type	Model	Variation of Shear Reinforcement (Stirrup)	Reinforcement Dimension
NC	S3	NC-S3	H and D	D10, s =100 mm D12, length = 175 mm
SCC	S1	SCC-S1	H	D10, s = 100 mm
SCC	S2	SCC-S2	D	D12, length = 175 mm
SCC	S3	SCC-S3	H and D	D10, s = 100 mm D12, length = 175 mm

Note: H: horizontal; D: diagonal

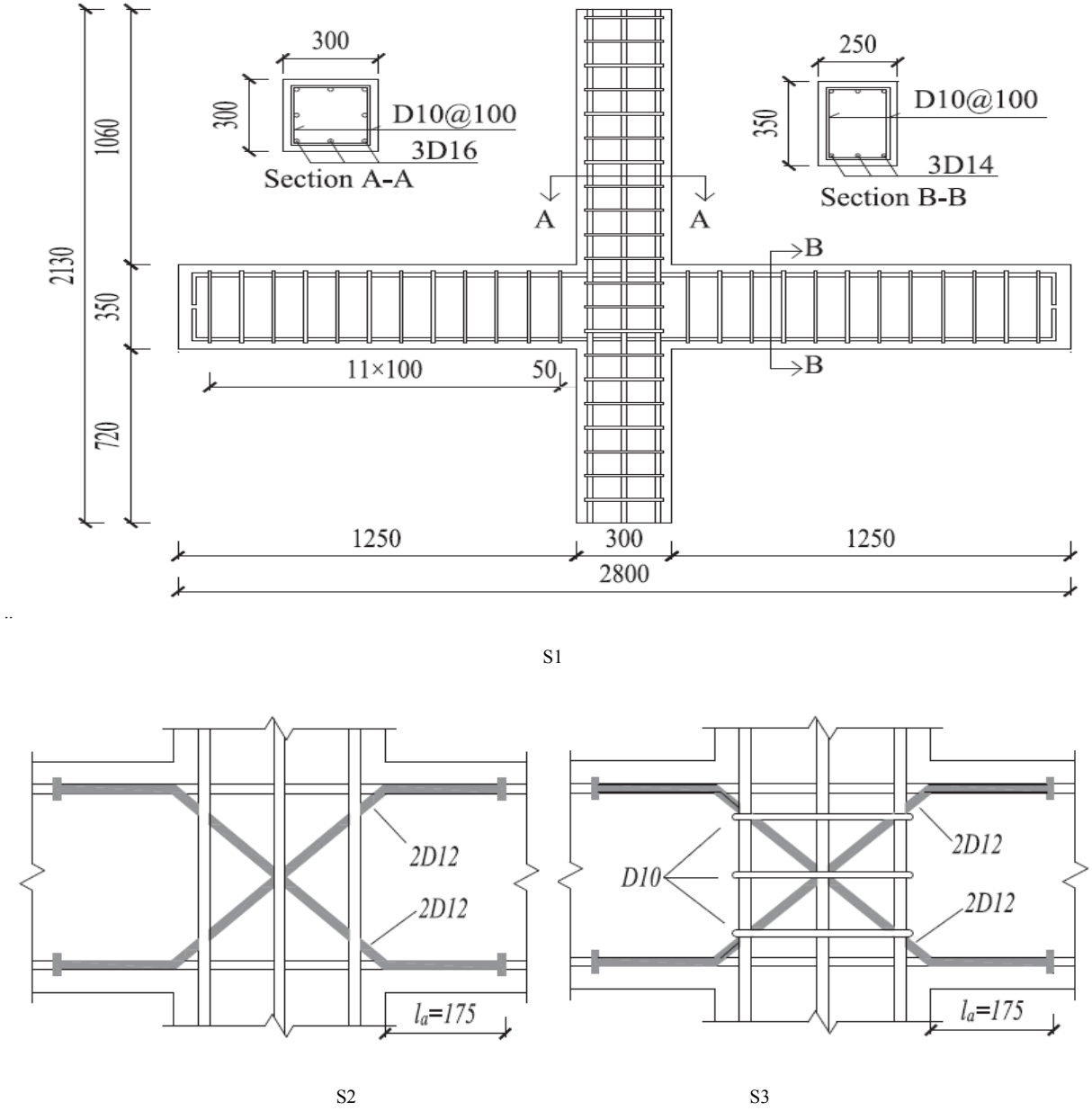

Figure 1. Details of shear reinforcement variations [11]

2.2. Structural Modeling Using the FEM

Nodes connected the structural element models in the Cartesian axis. The modeling of the IBC joint structures in this study was conducted using ANSYS software and based on FEM. The commands of software input were written in notepad files. The concrete, steel plates, and steel bars were represented by SOLID65, SOLID45, and LINK180 elements, respectively [19]. Figures 2 to 4 show the variation of shear reinforcement in the joint zones, and Figure 5 shows CONTA178 elements that represent the bond-slip interfaces. Determination of the size of elements greatly affects the accuracy of the analysis. Smaller mesh sizes produce more accurate analysis. Some non-linear equations were solved to obtain deformation [20, 21].

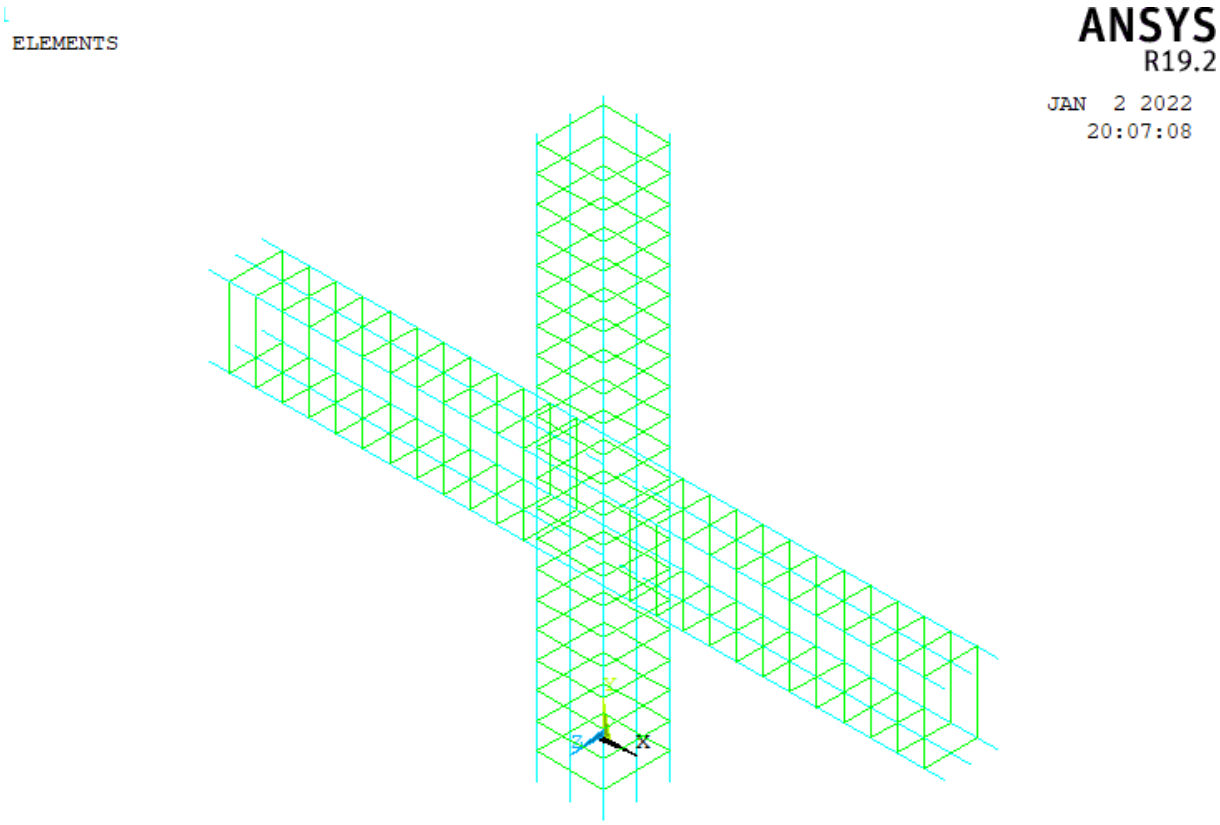

Figure 2. Steel bars model using LINK180 elements of the SCC-S1 model

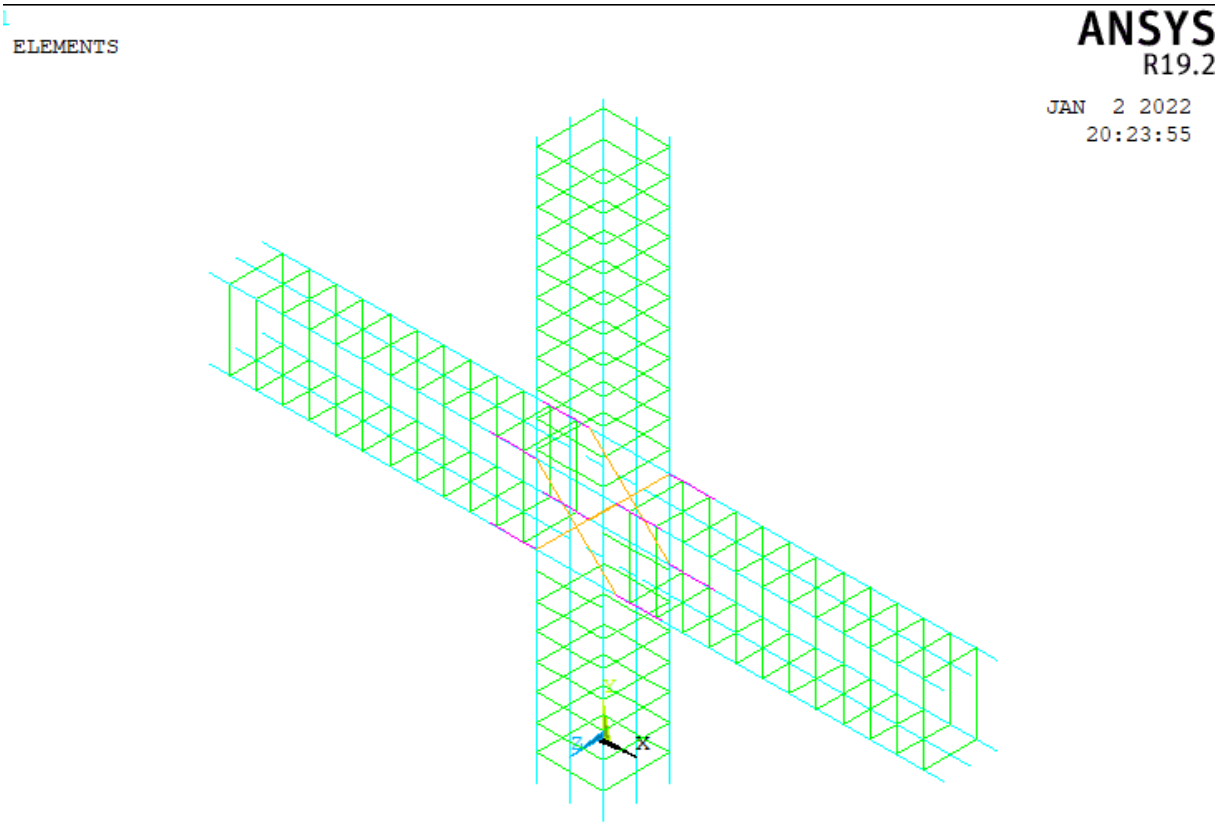

Figure 3. Steel bars model using LINK180 elements of the SCC-S2 model

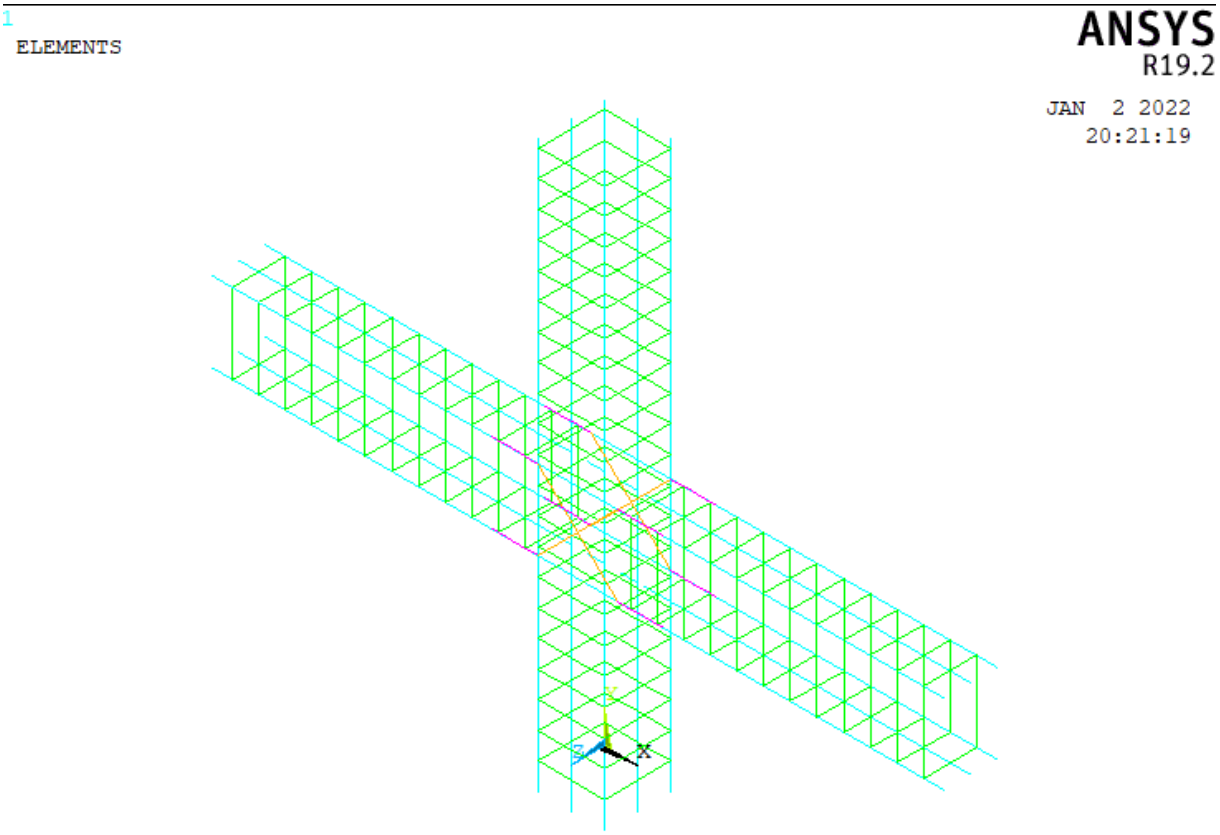

Figure 4. Steel bars model using LINK180 elements of the NC-S3 and SCC-S3 models

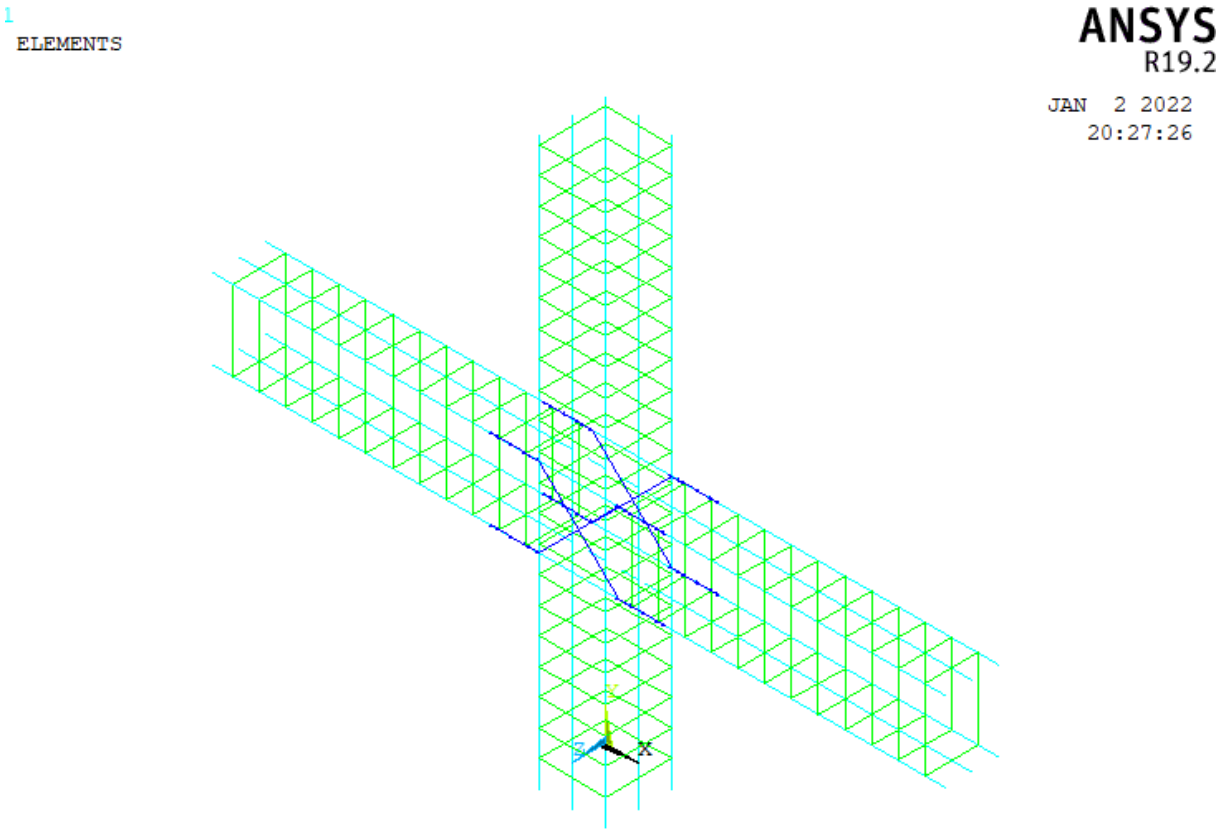

Figure 5. The bond-slip interfaces using CONTA178 elements (blue color)

2.3. Loading

The loads applied on the IBC joint structural elements were a combination of axial and lateral cyclic. The applied axial load was constant on $0{,}2f_c'A_g$ and the lateral cyclic load in Figure 6 was based on displacement control in the code [22].

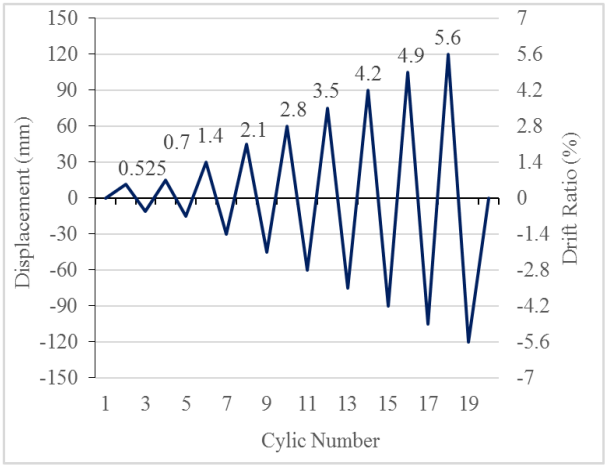

Figure 6. Loading cycle [20]

3. Results and Discussion

3.1. Interior Beam-Column Joint Using the Normal Concrete Material Model for Modeling Verification

The experimental works of IBC joint specimens [11] were modeled and analyzed based on the Finite Element Method (FEM) using ANSYS software. For modeling verification, the hysteresis curves of the experiment results of the NC-S3 specimen had been compared with the NC-S3 model. The materials were Normal Concrete for both specimen and model. The difference between the maximum lateral loads of the experiment and model under the push and pull cyclic lateral load directions were 6.602% and 9.869%, respectively. These differences were less than 10%, so they were included in the accuracy [23]. In the input of the FEM model, the displacements both in pull and push cyclic lateral load directions were set the same with the experiments.

The cause of this difference was that the displacement value in ANSYS was greater than the experimental test due to the non-linear equations reaching convergence on the determined displacement value, as is shown in Figure 7. The difference between the maximum lateral loads and displacements of experimental and FEM model results is shown in Table 3.

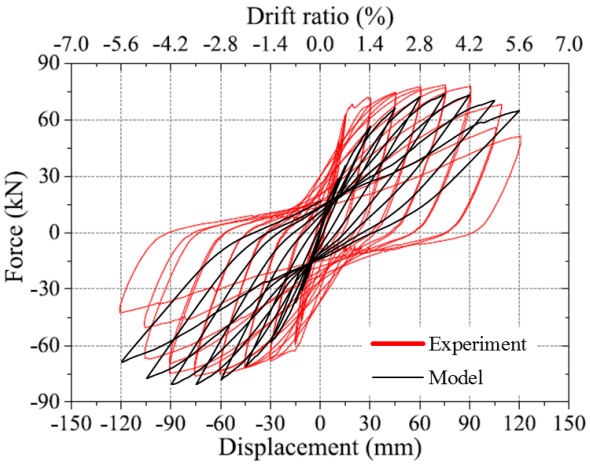

Figure 7. Hysteresis curves of experiment and model

In structural elements using Normal Concrete, the stress that occurred due to the application of cyclic lateral loads could be greater than the yield stress. This was because the structural elements received a large load so that the structure experienced yielding. The results of the ANSYS analysis in the form of structural element stresses for IBC joints under push and pull cyclic lateral load directions are shown in Figures 8 and 9.

Table 3. Variation of shear reinforcement

Load direction	Experiment		Model		Difference
	Max. lateral load	Displacement	Max. lateral load	Displacement	
	(kN)	(mm)	(kN)	(mm)	(%)
Push (+)	78.50	75.00	73.32	76.76	6.60
Pull (-)	76.20	75.00	83.67	76.71	9.87

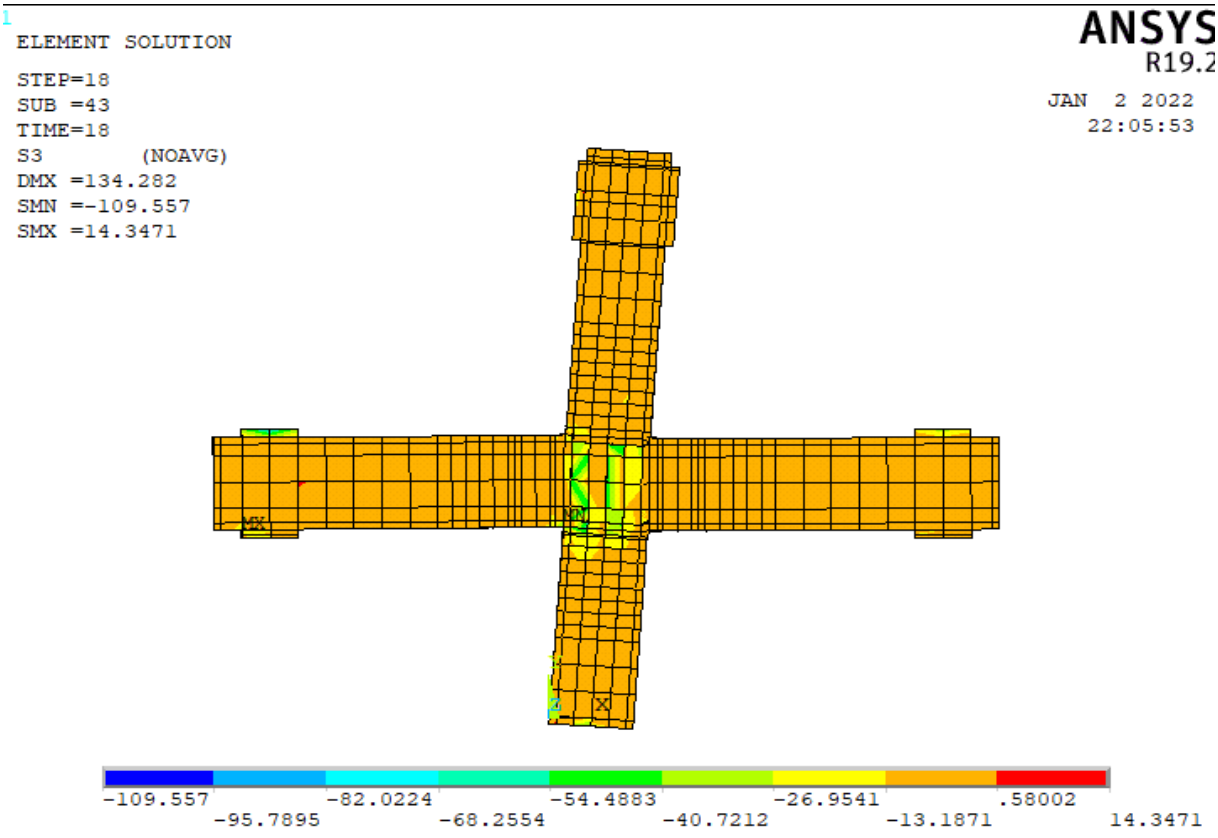

Figure 8. Stress contour of Normal Concrete-S3 IBC joint in drift ratio of 5.6% under push load

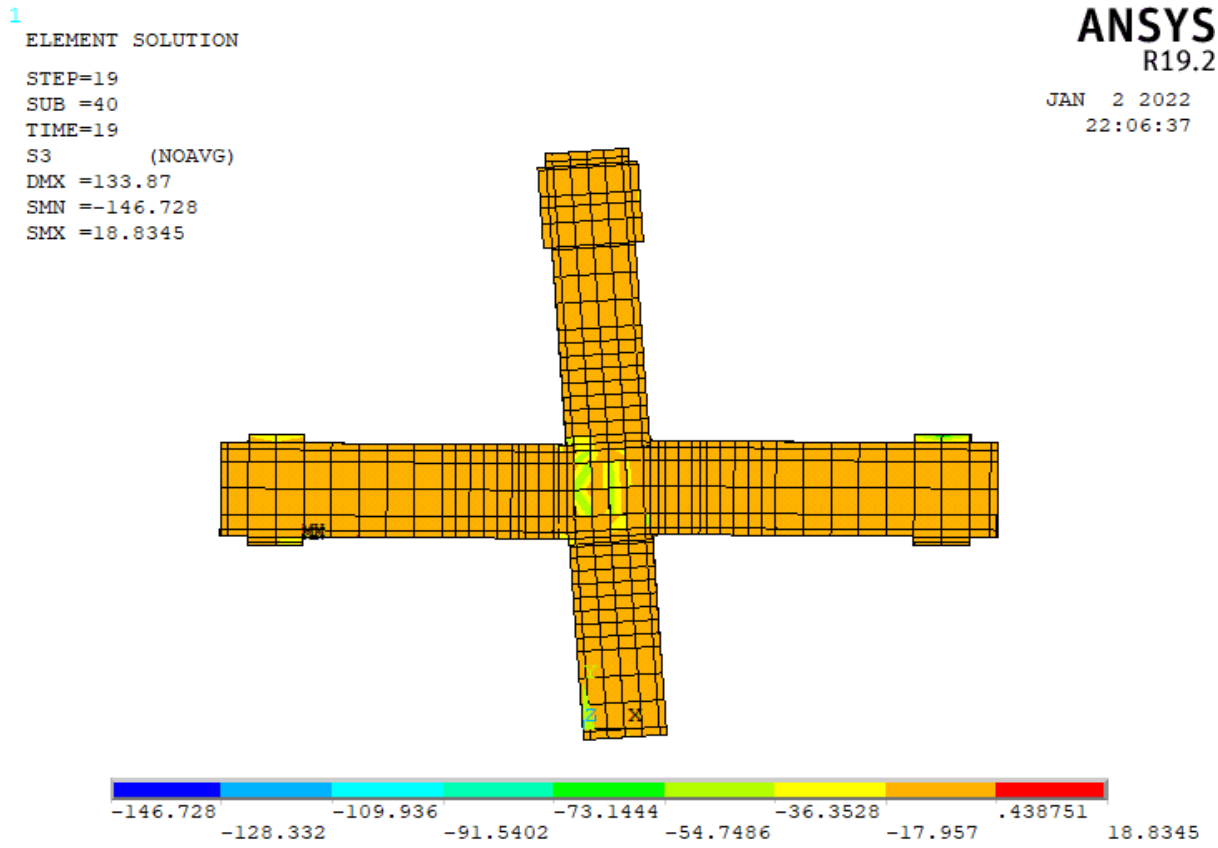

Figure 9. Stress contour of Normal Concrete-S3 IBC joint in drift ratio of 5.6% under pull load

3.2. Models of Interior Beam-Column Joint Using Self-Compacting Concrete

The three other models of IBC joint used data of Self-Compacting Concrete material with properties based on the previous research [17]. Then, the values of constant axial load were changed (2). The concrete compressive strength (f_c' in MPa) and gross area of the column section (A_g in mm^2) were used to determine the constant axial loads on the columns.

$$0{,}2\, f_c' A_g \quad (2)$$

There were three types of shear reinforcements in the joint zones, namely S1, S2, and S3. Because each model has specific detail of shear reinforcement in the joint zone, there are different lateral loads (strengths) and displacements on the hysteretic curves in Figures 10 (a), (b), and (c). Based on these hysteresis curves, the maximum lateral load and displacement values are shown in Table 4. The value of the drift ratios at the maximum lateral loads is described in Table 5.

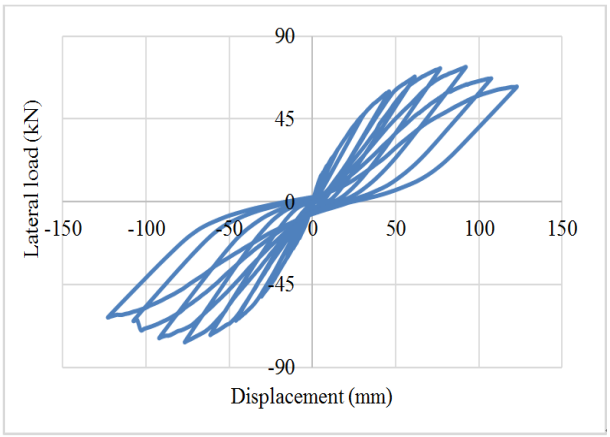

(a) Type SCC-S1 joint reinforcement

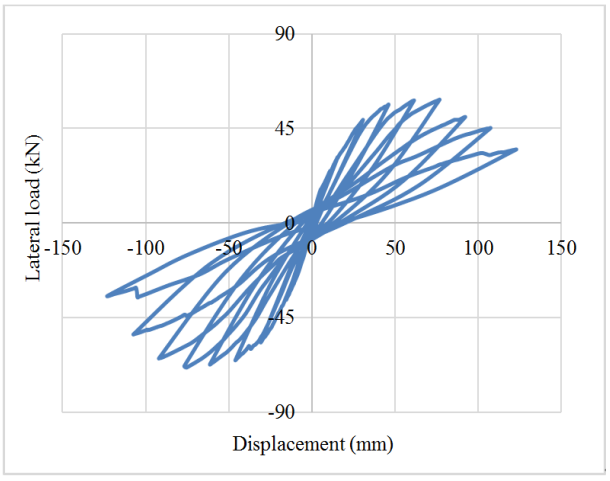

(b) Type SCC-S2 joint reinforcement

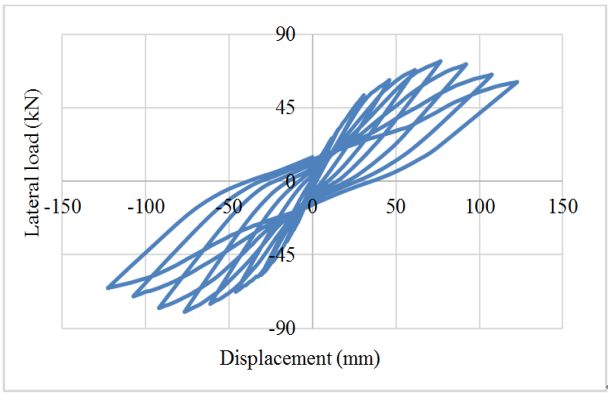

(c) Type SCC-S3 joint reinforcement

Figure 10. The hysteretic curve of interior beam-column joint models using Self-Compacting Concrete

Table 4. Maximum values of lateral load and displacement of type SCC-S1, SCC-S2, and SCC-S3 shear reinforcement of interior BCS

Type	Max. lateral load (kN)	Displacement (mm)	Load direction
SCC-S1	73.12	92.13	Push
	74.01	92.16	Pull
SCC-S2	58.74	76.78	Push
	67.97	76.72	Pull
SCC-S3	73.42	76.76	Push
	79.81	76.72	Pull

Table 5. Drift ratio in the maximum lateral load

Load direction	Drift ratio (%)		
	SCC-S1	SCC-S2	SCC-S3
Push	4.2	3.5	3.5
Pull	3.5	3.5	3.5

The element stress contours of the SCC-S1, SCC-S2, and SCC-S3 types of Interior Beam-Column joint models under the push and pull loads are shown in Figures 11 to 16. In the joint zones of the SCC-S1 and SCC-S3 models, horizontal stirrups confined the concrete and made the stress achieve compressive stress of (-)50 MPa to a tensile stress of 3.33 MPa. The joint zone area of the SCC-S3 type model that resisted compressive stress of (-)50 MPa was larger than the SCC-S1 type model due to the additional strength of the diagonal stirrups. In comparison, the SCC-S2 type model was only able to withstand compressive stress of (-)23.33 MPa to tensile stress of 3.33 MPa. The SCC-S2 type model only had diagonal stirrups and no horizontal stirrups to confine the concrete in the joint zone area. The lack of this type of reinforcement made it vulnerable to shear failure [24].

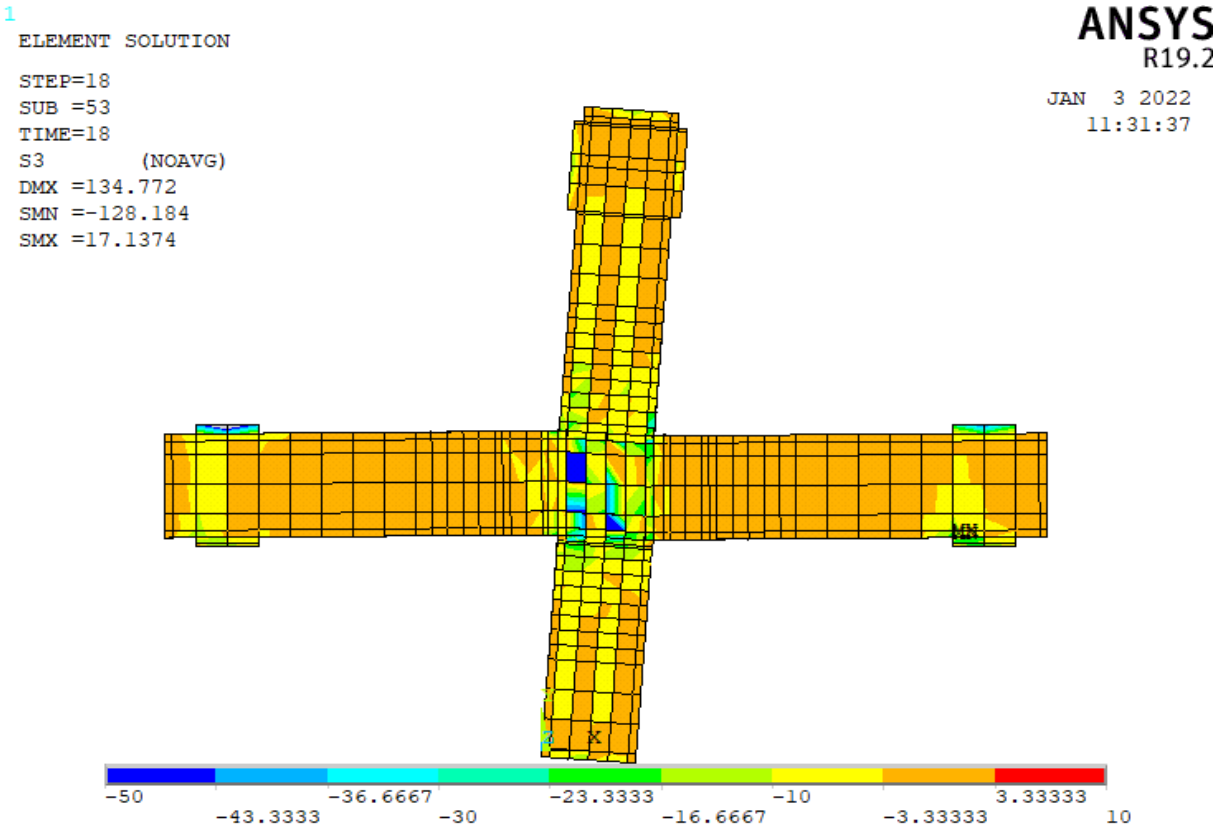

Figure 11. Stress contours of SCC-S1 type model on 5.6% drift ratio under push load

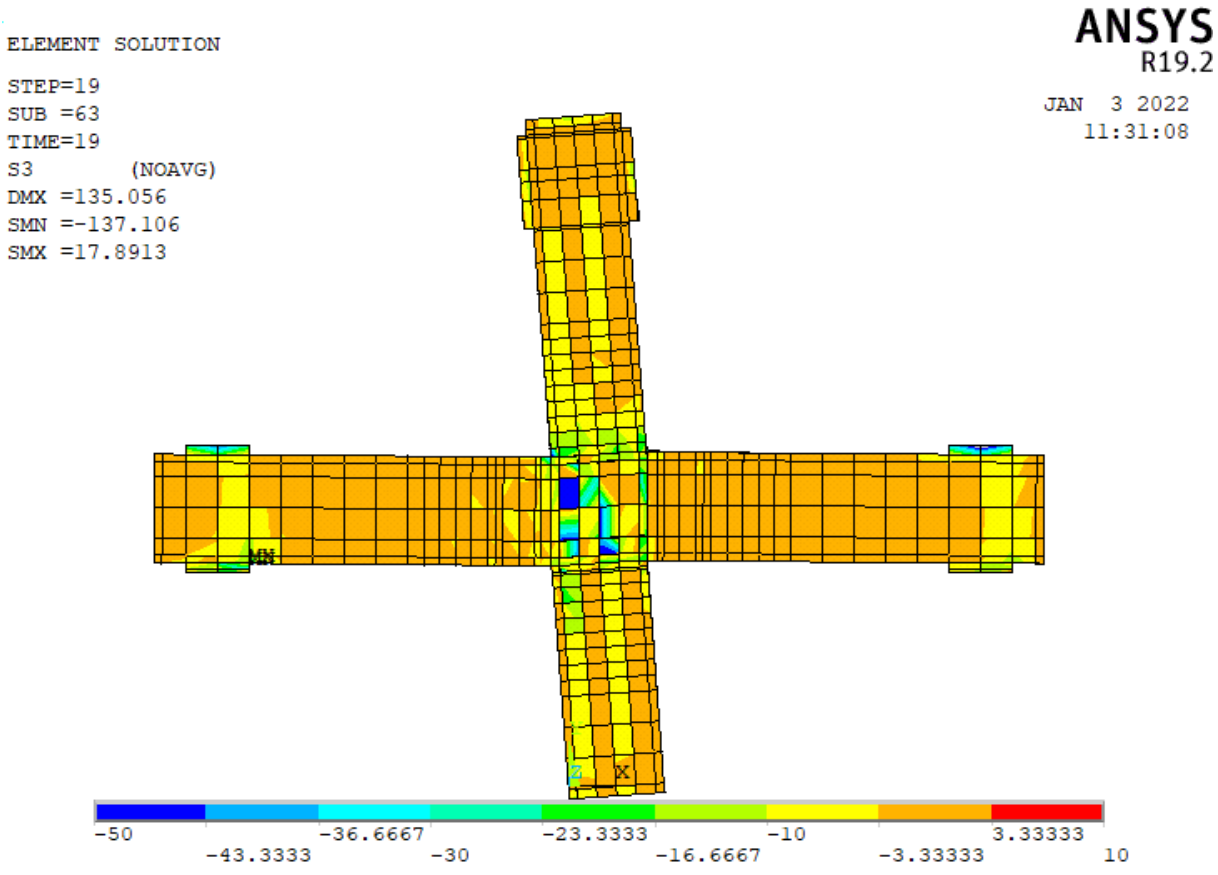

Figure 12. Stress contours of SCC-S1 type model on 5.6% drift ratio under pull load

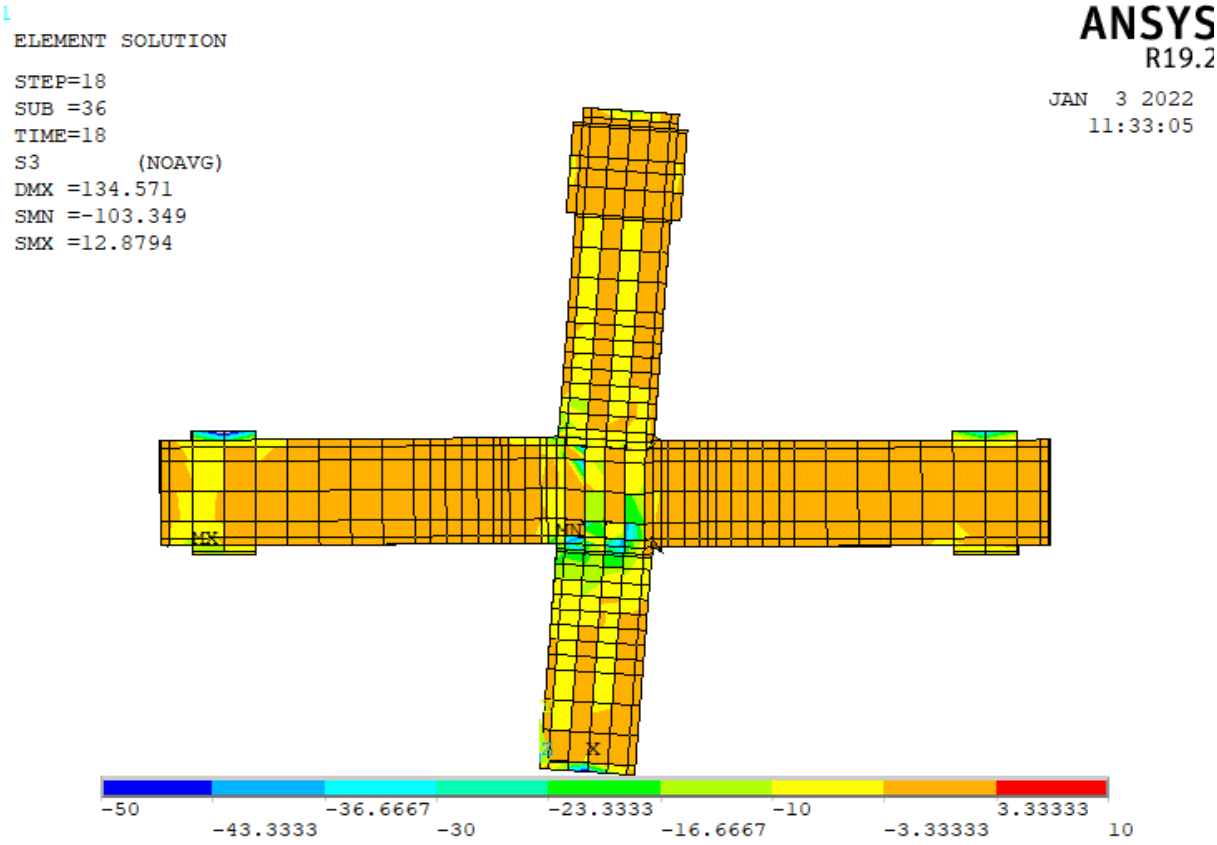

Figure 13. Stress contours of SCC-S2 type model on 5.6% drift ratio under push load

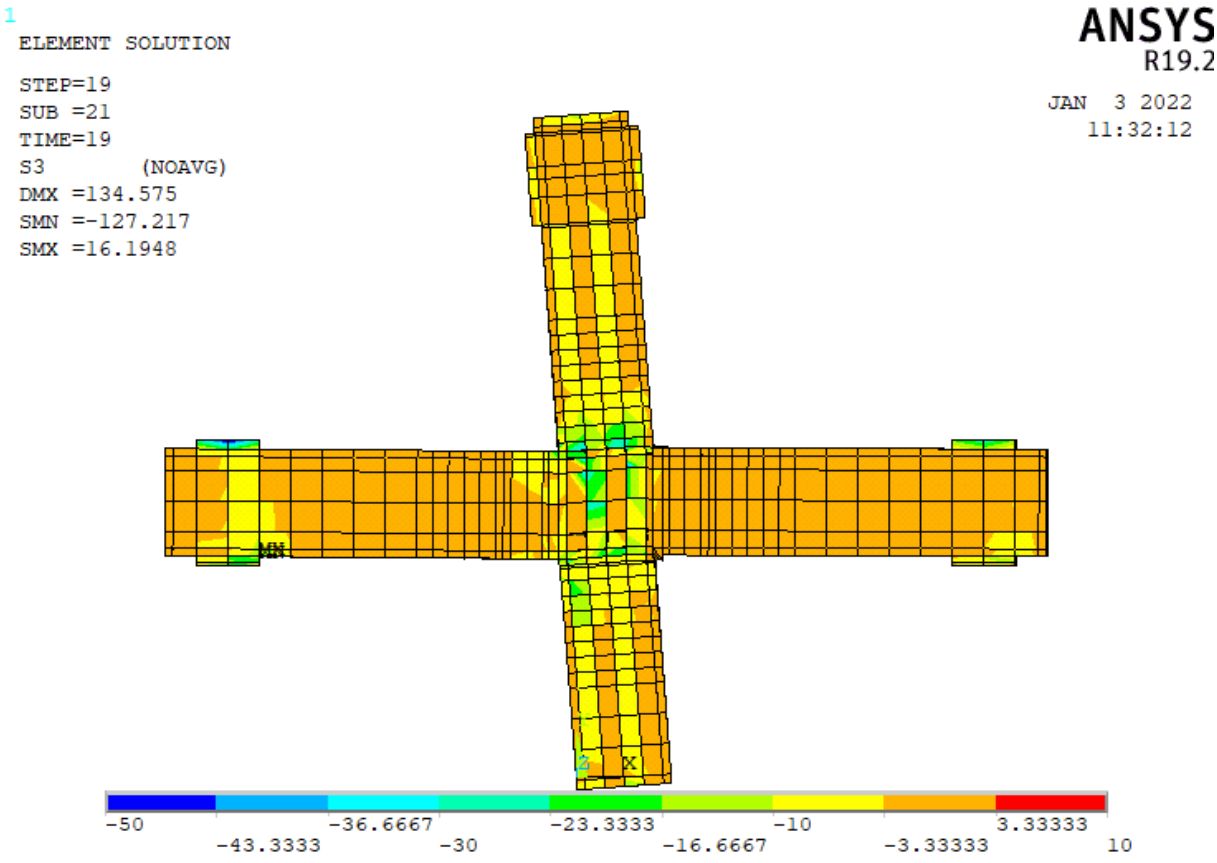

Figure 14. Stress contours of SCC-S2 type model on 5.6% drift ratio under pull load

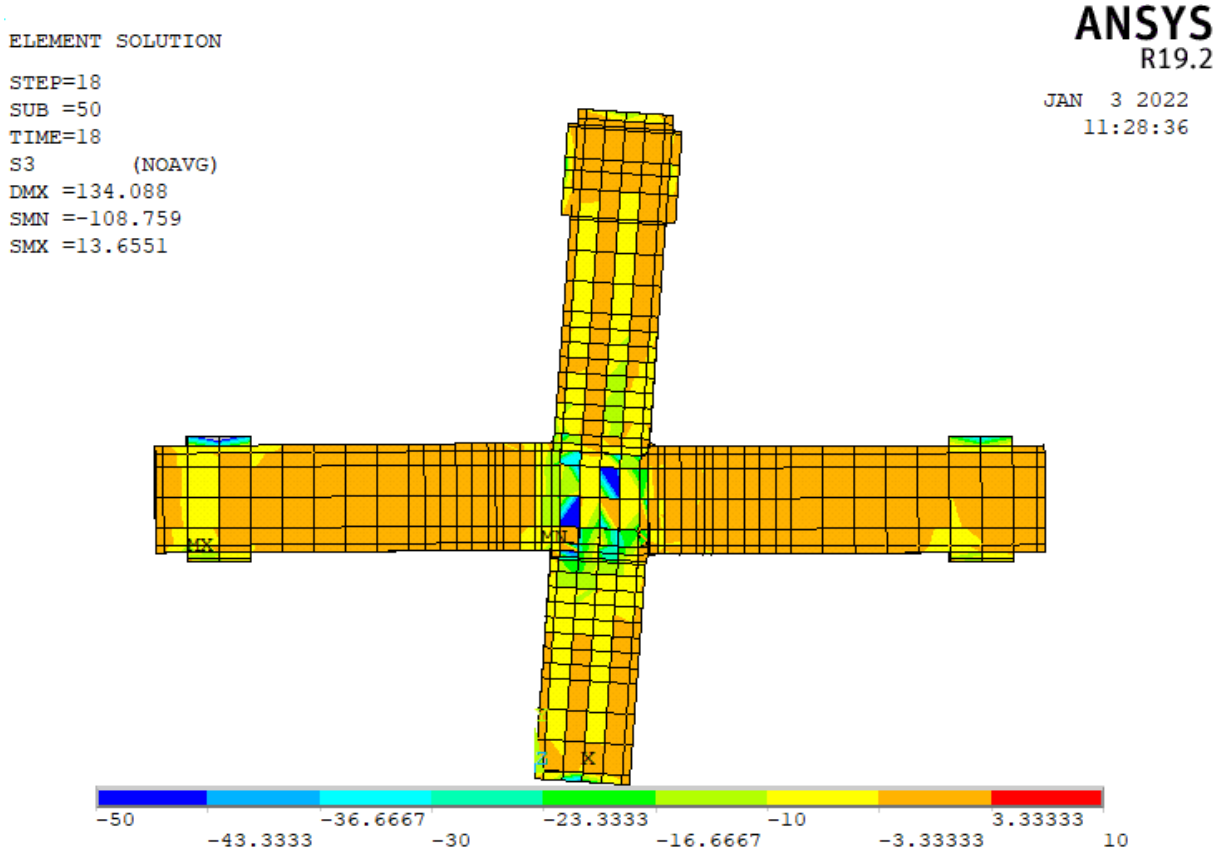

Figure 15. Stress contours of SCC-S3 type model on 5.6% drift ratio under push load

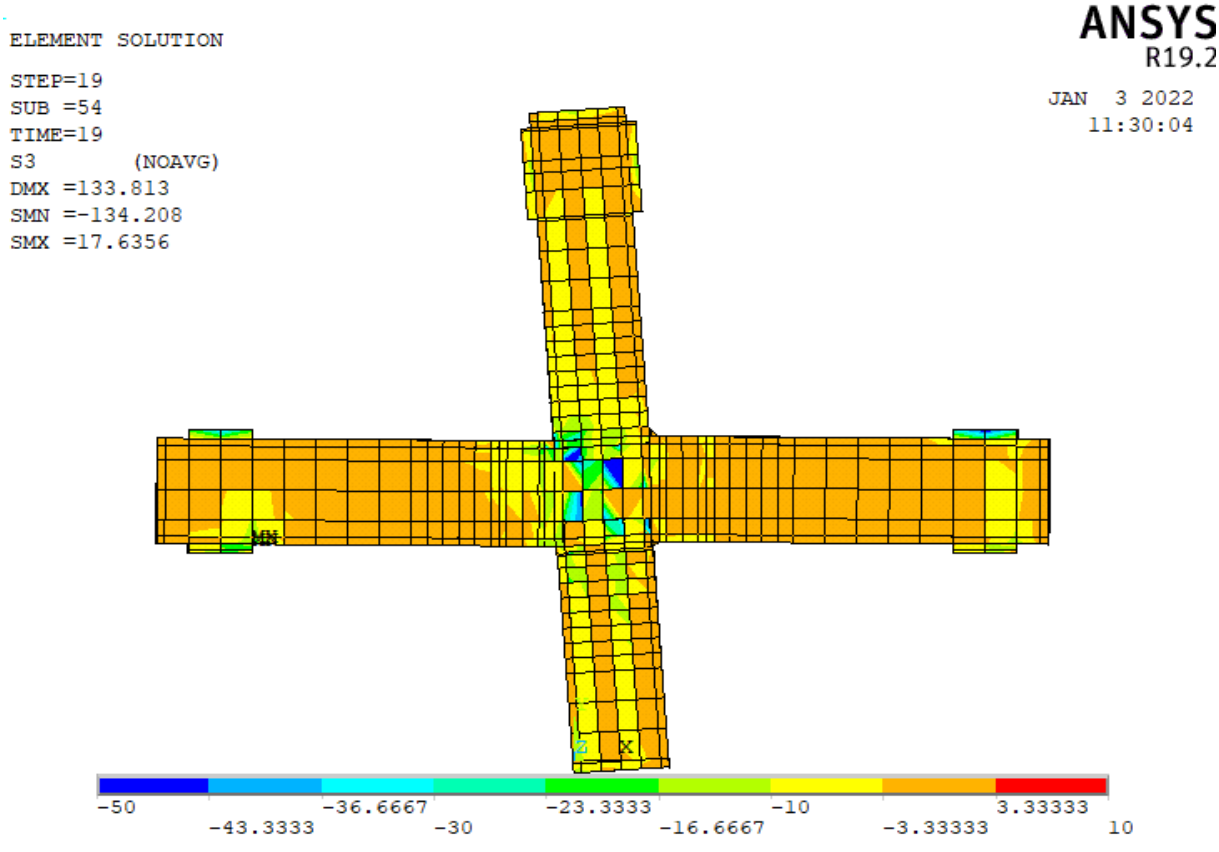

Figure 16. Stress contours of SCC-S3 type model on 5.6% drift ratio under pull load

3.3. Displacement Ductility

The ductile behavior of the structures can be determined from the ductility values. There are four types of ductility, namely displacement, curvature, rotational and strain ductility. The displacement ductility was used to analyze the effect of the type of shear reinforcement in the joint zones. The deformation at the ultimate to yield condition was compared to obtain the ductility value [25]. The area equation method was used based on the provision to determine the yield points [13]. It required the same relative areas on the upper and lower backbone curves, as is described in Figure 17. Since the ultimate and yield displacement values were determined, then the ductility values due to push and pull lateral cyclic loads could be calculated and shown in Table 6.

The average deformation ductility of the Normal Concrete (NC) Interior Beam-Column (IBC) joint model was 2.84. According to the provision [13], it was included in the moderate ductility demand with a value range of 2 to 4. The NC IBC joint model had horizontal and diagonal stirrup reinforcements that made the concrete of the joint more confined. This condition caused the model not to reach a high ductility higher than 4.

All IBC joint models using SCC materials with various types of joint reinforcement SCC-S1, SCC-S2, and SCC-S3 also achieved moderate ductility in a range of 2 to 4. The SCC-S1 model with horizontal shear reinforcement had the smallest ductility value of 2.41 because the model was more rigid, and there was a slip on the interfaces of the concrete and steel bars. When reaching the maximum lateral force, the drift ratio of the loading direction of the push was greater than that of the pull.

The SCC-S2 model has the highest ductility value than the SCC-S1 and SCC-S3 models. This different ductility value was because the SCC-S2 model only had diagonal reinforcements at the joint. It caused the structure to yield faster than the SCC-S1 and SCC-S3 models. While the SCC-S3 model had horizontal and diagonal shear reinforcements, the concrete in the joint of this model was more confined. The beam-column joint interior structure is expected to withstand moderate earthquake loads with moderate ductility. As is well known, ductility is significant in supporting a well-behaved structure in dissipating earthquake energy [26].

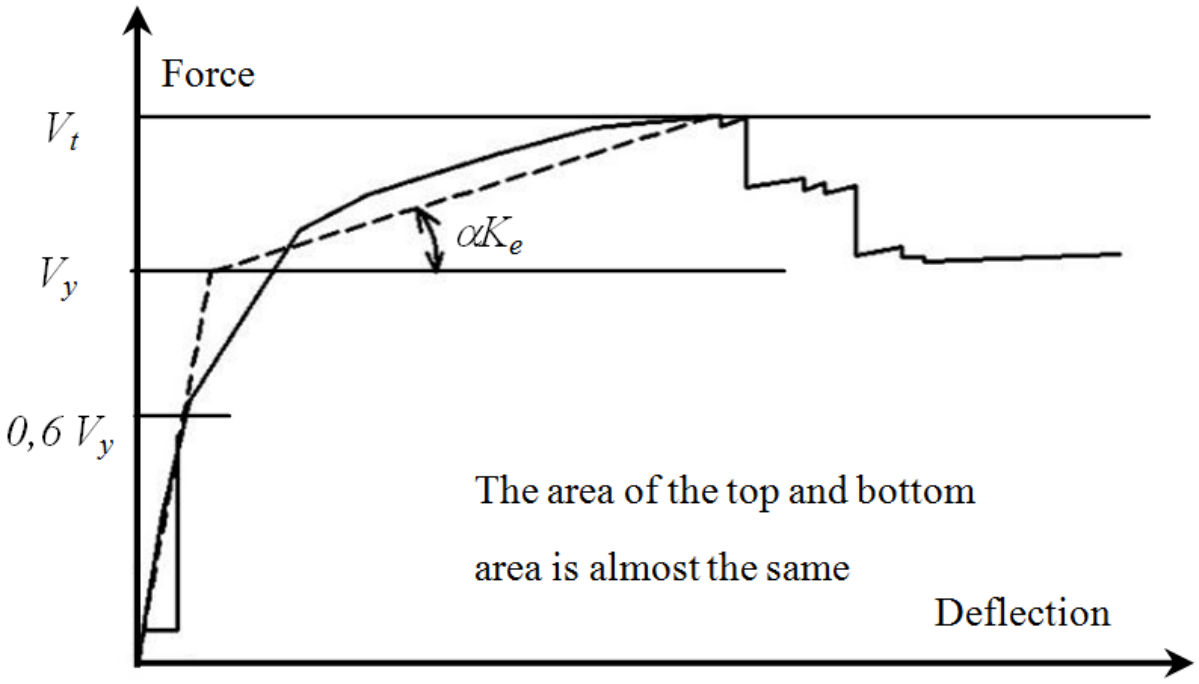

Figure 17. Determination of yield point (positive post-yield slope) [13]

Table 6. Displacement ductility values of the interior Beam-Column Joint model using Normal Concrete and Self Compacting Concrete with Various Joint Reinforcement

Type	Mate-rial	Load direction	Max. displacement	Yield displacement	Displacement ductility	Average ductility
			Δu	Δy	μ	$\bar{\mu}$
			(mm)	(mm)		
			(1)	(2)	(3) = (2)/(1)	
S3	NC	Push	122.77	42.53	2.89	2.84
		Pull	122.69	43.97	2.79	
S1	SCC	Push	122.86	52.35	2.35	2.41
		Pull	122.91	49.56	2.48	
S2	SCC	Push	122.83	35.85	3.43	3.44
		Pull	122.82	35.63	3.45	
S3	SCC	Push	122.73	48.09	2.55	2.59
		Pull	122.68	46.68	2.63	

3.4. Stiffness and Strength

The stiffness value in the structure is obtained from the ratio of the lateral force (lateral load or strength) to the displacement at a certain drift ratio. The correlation between the stiffness and the drift ratio can be depicted in a curve under push and pull cyclic lateral load directions. This curve shows how the stiffness degradation of the structure model due to the applied loads until the last drift ratio. The stiffness value in the structure was obtained from the ratio of the lateral load to the displacement at certain drift ratios (1). Commonly, stiffness and strength are closely related to the shear reinforcement of beams, columns, and joint zones [27]. The lack of shear reinforcement to confine the concrete in the joint zone can rapidly degrade stiffness and strength due to cyclic lateral loads.

Figure 18 shows the correlation curve of stiffness degradation and drift ratio of the Interior Beam-Column joints type S1, S2, and S3 models using NC and SCC materials. In the initial story drift of the push direction, the NC-S3 model had the highest stiffness of 2.405 kN/mm, followed by the SCC-S3, SCC-SCC-S2, and SCC-S1 models with stiffnesses of 2.286, 2.166, and 2.052 kN/mm, respectively. This behavior was because the NC-S3 and SCC-S3 models had horizontal and diagonal stirrup reinforcement in the joint zone that provided more stiffness. When the story drift reached 2.1%, the behavior changed, where models SCC-S1 and SCC-S3 showed almost similar stiffness degradation of 1.3000 and 1.343 kN/mm. It was because both models had horizontal stirrup reinforcement that confined the joint zone. This behavior continued until it reached a story drift of 5.6%. Figure 19 shows the stiffness degradation of all these models in the pull direction. In the initial story drift of the pull loading, the NC-S3 showed the maximum stiffness of 2.827 kN/mm, followed by SCC-S3, SCC-S2, and SCC-S1 models with values of 2.600, 2.600, and 2.196 kN/mm, respectively. This behavior changed when it reached a story drift of 2.8%. The SCC-S2 model experienced stiffness degradation faster to 1.417 kN/mm than the other three models due to the absence of horizontal stirrups as joint zone restraints [28] according to the code [29]. The behavior of the NC-S3 models under push and pull loads showed that in the initial condition, the NC material performed higher stiffness than SCC material.

The strength degradation was due to the inability of the structure model to resist the applied push and pull directions loads. The increasing number of load cycles will reduce the stiffness of the structure. The stiffness degradation was also due to the drift ratio and the detail of joint reinforcement modeling.

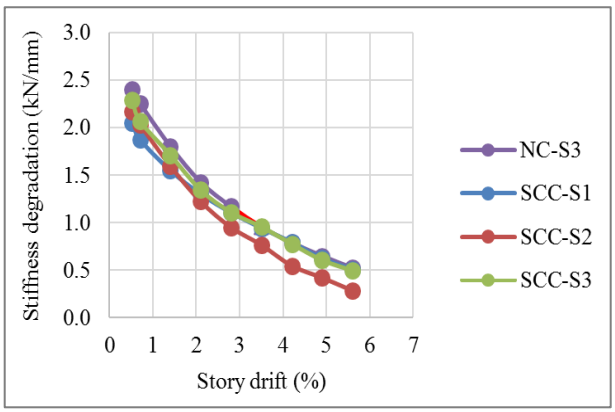

Figure 18. Curves of stiffness degradation and story drift correlation under push load directions of NC-S3, SCC-S1, SCC-S2, and SCC-S3 interior beam-column joints

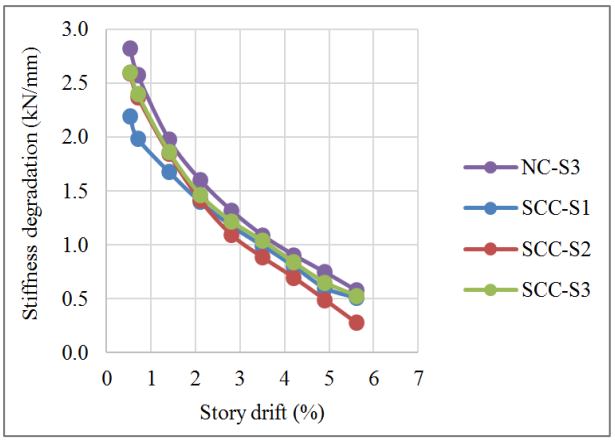

Figure 19. Curves of stiffness degradation and story drift correlation under pull load directions of NC-S3, SCC-S1, SCC-S2, and SCC-S3 interior beam-column joints

4. Conclusions

The analysis based on FEM on four interior Beam-Column Joints using Normal Concrete and Self-Compacting Concrete with various joint reinforcements leads to conclusions as follows:

1. Numerical modeling of interior column beam joints subjected to lateral cyclic loads produced hysteretic curves with a difference of each lateral load less than 10% compared with the experiment. Then it met the accuracy requirements. The different percentages of maximum lateral forces under push and pull loads were 6.602% and 9.869%, respectively.
2. The SCC-S3 numerical model of beam-column connection using Self Compacting Concrete (SCC) material achieved the highest lateral force compared to the other two models. This performance was due to horizontal and diagonal stirrup reinforcements in the joint zone that confined concrete and resisted tensile and compressive forces due to cyclic lateral loads. Only horizontal hoop reinforcements provided in the SCC-S1 model could withstand smaller lateral forces than the SCC-S3 model. The SCC-S2 model could withstand the smallest cyclic lateral forces because it only had diagonal stirrups to withstand the axial tension and compression forces. There were no horizontal stirrups to confine the concrete in the joint zone.
3. The SCC-S2 model experienced the fastest structural yield because it only had diagonal stirrup reinforcements without horizontal stirrup reinforcements to confine the concrete in the joint zone. It made the joint deformed further than other models and achieved the highest ductility value of 3.437. This model also showed the smallest stress values in the stress contour under push and pull loads. The concrete cracks, which are usually diagonal in the joint zone, could be minimized by using diagonal shear reinforcement of the SCC-S2 model. The SCC-S1 and SCC-S3 models reached structural yields slower than the SCC-S2 model, so they performed less ductility. However, all models had ductility values in the medium category.
4. All models of Beam-Column Joints using Self Compacting Concrete material experienced stiffness degradation along with the increased story drifts. Since the story drift was 2.1% (push load) and 2.8% (pull load), the SCC-S1 and SCC-S3 models experienced almost the same strength (load) degradation because they had horizontal stirrups in the joint zone to confine the concrete. The SCC-S2 model degraded the fastest because no horizontal stirrups provide stiffness in the joint zone.
5. Based on the area and value of stress contour, the interior BCJ SCC-S3 model with horizontal and diagonal shear reinforcements achieved the highest lateral forces and resisted compressive stresses of (-) 50 MPa and tensile stresses 3.33 MPa in the largest area and better stiffness degradation than other models.
6. The SCC-S2 interior BCS model achieved the highest ductility value of 3.437 because of the faster structure yield due to diagonal shear without horizontal reinforcement in the joint zone.
7. Overall, the SCC-S1 and SCC-S3 models using Self-Compacting Concrete material showed the ability to resist cyclic lateral forces well and significantly affect the structure's performance. The inability of the SCC-S2 model to maintain stiffness is due to not having horizontal stirrups in the joint zone. The results showed that the SCC-S3 interior BCJ with a combination of horizontal and diagonal shear reinforcements performed the best performance among all SCC IBC joints.

Acknowledgments

All the authors would thank Sriwijaya University for supporting the study presented in this article.

REFERENCES

[1] Lu, X., Urukap, T.H. Li, S., and Lin, F. Seismic Behavior of Interior RC Beam-Column Joints with Additional Bars Under Cyclic Loading, Earthquake and Structures, Vol. 3. No. 1, 37–57, 2012. https://doi.org/10.12989/eas.2012.3.1.037

[2] Ganesan, N., Nidhi, M., and Indira, P.V. SFRHPC Interior Beam-Column-Slab Joints Under Reverse Cyclic Loading, Advances in Concrete Construction, 3(3), 237–250, 2015. http://dx.doi.org/10.12989/acc.2015.3.3.237

[3] European Federations. The European Guidelines for

Self-Compacting Concrete: Specification, Production, and Use, European, 2005.

[4] Ashtiani, M.S., Dhakal, M.P., and Scott, A.N. Seismic Performance of High-Strength Self-Compacting Concrete in Reinforced Concrete Beam-Column Joints, Journal of Structural Engineering, Vol. 140 No. 5, 2014. https://doi.org/10.1061/(ASCE)ST.1943-541X.0000973

[5] Mobin, S.J. Cyclic Behaviour of Interior Reinforced Concrete Beam-Column Connection with Self-Consolidating Concrete, Structural Concrete, Vol. 17, No. 4, 618-629, 2016. https://doi.org/10.1002/suco.201500133

[6] Hu, B. and Kundu, T. Seismic Performance of Interior and Exterior Beam–Column Joints in Recycled Aggregate Concrete Frames, Journal of Structural Engineering, Vol. 145, No. 3, 2019. https://doi.org/10.1061/(ASCE)ST.1943-541X.0002261

[7] Patrisia, Y. Self Compacting Concrete Using Fly Ash and Dust Stone as Filler Material, Journal Balanga, Vol. 2, No. 1, 70–80, 2014.

[8] National Standardization Board, SNI 2847-2019 Procedure for Calculation of Concrete Structures for Buildings, Jakarta, 2019. (in Indonesian)

[9] Lee, S.W., Tan, K.H., and Yang, E-H. Seismic Behaviour of Interior Reinforced-Concrete Beam-Column Sub-Assemblages with Engineered Cementitious Composites, Magazine of Concrete Research, Vol. 70, No. 24, 1280–1296, 2018.https://doi.org/10.1680/jmacr.17.00359

[10] Feng, J., Wang, S., Meloni, M., Zhang, Q., Yang, J., and Cai, J. Seismic Behavior of RC Beam Column Joints with 600 MPa High Strength Steel Bars, Applied Sciences, Vol. 10, No. 13, 4684, 2020. https://doi.org/10.3390/app10134684

[11] Shen, X., Li, B., Chen. Y-T., and Tizani, W., Seismic Performance of Reinforced Concrete Interior Beam-Column Joints with Novel Reinforcement Detail, Engineering Structures, 227 (2021) 111408. https://doi.org/10.1016/j.engstruct.2020.111408

[12] Dietrich, M. Z., Calenzani, A. F. G., and Fakury, H. L. Analysis of rotational stiffness of steel-concrete composite beams for lateral torsional buckling, Engineering Structures, Vol. 198, No. 109554, 1-15, 2019. https://doi.org/10.1016/j.engstruct.2019.109554

[13] Federal Emergency Management Agency, FEMA 356 Prestandard and Commentary for the Seismic Rehabilitation of Buildings, Washington DC, 2000.

[14] Moaz, A. Finite Element Analysis is a Powerful Approach to Predictive Manufacturing Parameters, Journal of University of Babylon for Pure and Applied Sciences, Vol. 26, No. 1, 229-238, 2018.

[15] Thompson, M. K., and Thompson, J. M. ANSYS Mechanical APDL for Finite Element Analysis, Cambridge: Elsevier Inc., 2017.

[16] ANSYS, Inc. ANSYS Mechanical APDL Structural Analysis Guide, Canonsburg: SAS IP, Inc., 2019.

[17] Hanafiah, Saloma, and Whardani, P. N. K. The Behavior of Self-Compacting Concrete (SCC) with Bagasse Ash, AIP Conference Proceedings, Vol. 1903, No. 1, 10.1063/1.5011544, 2017. https://doi.org/10.1063/1.5011544

[18] China Building Industry Press. Code for design of concrete structures, GB50010, 2015th ed., Beijing: China Building Industry Press, 2015.

[19] ANSYS Inc. ANSYS Mechanical APDL Introductory Tutorials, United States of America, 2019.

[20] Agustina, A.F., Saloma, Nurjannah, S.A., Usman, A.P., and Hanafiah. Numerical analysis of the behavior of light concrete panels with variations of thickness and door opening position in resisting static monotonic loads, International Journal of Advanced Technology and Engineering Exploration, Vol. 7, No. 73, 201-219, 2020. http://dx.doi.org/10.19101/IJATEE.2020.762110

[21] Budiono, B., Nurjannah, S. A., and Imran, I. Nonlinear Numerical Modeling of Partially Pre-stressed Beam-column Sub-assemblages Made of Reactive Powder Concrete, Journal of Engineering and Technological Sciences, Vol. 51, No.1, 28-47, 2019. https://doi.org/10.5614/j.eng.technol.sci.2019.51.1.3

[22] ACI Committee 374. ACI 374.1-05 Acceptance Criteria for Moment Frames Based on Structural Testing and Commentary, American Concrete Institute, Farmington Hills, MI, 2019 (reapproved).

[23] Badshah, M., Badshah, S., and Jan, S. Comparison of computational fluid dynamics and fluid structure interaction models for the performance prediction of tidal current turbines, Journal of Ocean Engineering and Science, Vol. 5, No. 2, 164-172, 2020. https://doi.org/10.1016/j.joes.2019.10.001

[24] Dang, C. T. and Dinh, N. H., Experimental Study on the Structural Performance of Beam-Column Joints in Old Buildings without Designed Shear Reinforcement under Earthquake, Materials Science Forum, 902, 33-40, 2017. https://doi.org/10.4028/www.scientific.net/MSF.902.33

[25] Nurjannah, S. A., Budiono, B., and Imran, I. Influence of Partial Prestressing Ratio on Hysteretic Behavior of Beam Column Subassemblage Using Reactive Powder Concrete Materials, International Journal of Scientific & Technology Research, Vol. 9, No. 2, 1933-1941, 2020.

[26] Isler, O. Seismic Performances and Typical Damages of Beam-Column Joints in the RC Buildings, The 14th World Conference on Earthquake Engineering, Beijing, 1-6, 2008.

[27] El-Naqeeb, M. H., Abdelwahed, B. S., El-Metwally, S. E. Numerical investigation of RC exterior beam-column connection with different joint reinforcement detailing, Structures, 38, 1570–1581, 2022. https://doi.org/10.1016/j.istruc.2022.03.014

[28] Gautham, A. and Sahoo, D. R., Performance of SRC column-RC beam joints under combined axial and cyclic lateral loadings, Engineering Structures, 260, 114218, 1-16, 2022. https://doi.org/10.1016/j.engstruct.2022.114218

[29] ACI 318-19 Committee. Building code requirements for structural concrete (ACI 318-19) and commentary. American Concrete Institute, Farmington Hills, Michigan, 2019.